Available on the CERN CDS information server **CMS PAS HIN-15-002**

CMS Physics Analysis Summary

Contact: cms-pag-conveners-heavyions@cern.ch 2015/07/13

Study of Z boson production in pPb collisions at $\sqrt{s_{NN}} = 5.02$ TeV

The CMS Collaboration

Abstract

The electroweak boson production is an important benchmark measurement in ultra-relativistic heavy-ion collisions which can provide constraints on the nuclear modification of parton distribution functions. In this paper the results from the proton-lead collision data taken in early 2013 are presented. The Z boson production is studied in the electron and muon decay channels. The cross section is measured in bins of the Z boson rapidity and transverse momentum and compared to theoretical predictions. The Z boson production is observed to be proportional to the number of elementary nucleon-nucleon collisions within the uncertainties. The forward-backward ratio of the measured cross section is presented.

1 Introduction

Electroweak boson production is an important benchmark measurement in high-energy particle physics. The Z and W boson production was studied at hadron and e^+e^- colliders extensively at various collision energies. The latest measurements at the Large Hadron Collider (LHC) [1–7] are well described by the Standard Model using higher-order perturbative quantum chromodynamics (QCD) and recent parton distribution functions (PDFs).

With its large center-of-mass energy and high luminosity, the LHC allows the study of Z and W production in heavy-ion collisions for the first time. Electroweak bosons are essentially unmodified by the hot and dense medium created in nucleus-nucleus collisions, and their leptonic decays are of particular interest since leptons pass through the medium without being affected by the strong interaction. Both Z and W productions were measured by the ATLAS [8, 9] and the CMS [10, 11] experiments using PbPb collision data taken in 2010 and 2011 at $\sqrt{s_{NN}} = 2.76$ TeV, confirming with a precision of about 10%, that the production cross section scales with the number of elementary nucleon-nucleon collisions.

However, in heavy-ion collisions, the production of electroweak bosons can be affected by the initial conditions of the collision. The free proton PDFs are expected to be modified for protons bound in the Pb nucleus, which together with the fact that the nucleus contains neutrons besides protons, can modify the observed cross sections compared to pp collisions. Various groups studied the nuclear modification of PDFs, and several results are available at next-to-leading order (NLO) precision in QCD [12–14]. The results are obtained by global fits to the available deep inelastic scattering and Drell-Yan data, which constrain the nuclear PDFs (nPDFs) in a limited region of parton longitudinal momentum fraction x and four-momentum transfer Q^2.

The production of electroweak bosons in proton-nucleus collisions at the LHC provides an opportunity to study the nPDFs in a high Q^2 and low x phase-space region that was never studied before [15]. The CMS experiment measured W boson production in pPb collisions for the first time [16]. Deviations from the current expectations of parton distribution functions were observed, showing the need for including W boson data in nuclear parton distribution global fits.

Different models estimate different amount of modifications of the Z production cross section (σ) versus rapidity (y) and transverse momentum (p_T) [17–21]. The rapidity distribution of Z bosons is sensitive to the parton content of the interacting nucleons. Consequently, the symmetric rapidity spectrum of Z bosons in the center-of mass frame of pp collisions is modified by nuclear effects [20], that can be quantified by the forward-backward ratio:

$$R_{FB}(y) = \frac{d\sigma(+y)/dy}{d\sigma(-y)/dy} \tag{1}$$

where by convention positive rapidity values correspond to the proton-going direction. The goal of this paper is to measure the Z production cross section in bins of rapidity and transverse momentum of the lepton pairs to help constraining the parton content of the nucleons. The measurement is based on the pPb data taken in the beginning of 2013 and Z boson decays to muons or electrons.

2 Experimental methods

A detailed description of the CMS detector and its coordinate system can be found elsewhere [22]. Its central feature is a superconducting solenoid with internal diameter of 6 m, providing a magnetic field of 3.8 T. Within the superconducting solenoid volume are a silicon pixel and strip tracker, a lead tungstate crystal electromagnetic calorimeter, and a brass/scintillator hadron calorimeter. Electrons are measured in the ECAL that consists of 75 848 lead tungstate crystals providing a pseudorapidity coverage in the barrel region (EB) of $|\eta| < 1.48$ and in the two endcap regions (EE) of $1.48 < |\eta| < 3$. Muons are detected in the pseudorapidity range $|\eta| < 2.4$ using gas-ionization detectors embedded in the steel return yoke outside the solenoid. Extensive forward calorimetry complements the coverage provided by these barrel and endcap detectors.

The analysis is performed on the pPb collision data taken in the beginning of 2013 that correspond to an integrated luminosity of (34.6 ± 1.2) nb^{-1} [23]. Due to the LHC magnet system the beam energies were 4 TeV for protons and 1.58 TeV per nucleon for lead nuclei, resulting in a center-of-mass energy per nucleon pair of $\sqrt{s_{NN}} = 5.02$ TeV. As a result of the energy difference between the colliding beams, the nucleon-nucleon center-of-mass frame is not at rest with respect to the laboratory frame. Massless particles emitted at rapidity $y_{\text{c.m.}} = 0$ in the nucleon-nucleon center-of-mass frame will be detected at $y = -0.465$ (clockwise proton beam) or +0.465 (counterclockwise proton beam) in the laboratory frame. The results presented hereafter are expressed in the center-of-mass frame with the proton-going side defining the region of positive y values, to respect the usual convention of the proton fragmentation region being probed at positive rapidity. The direction of the higher energy proton beam was initially set up to be clockwise, and was then reversed splitting the data in two parts with comparable sizes.

During the data taking electron and muon triggers were employed to select events with high p_{T} leptons. The muon analysis is based on a sample triggered by requiring at least one muon with p_{T} above 12 GeV/c. The electron analysis is based on a photon or electron triggered sample requiring at least one ECAL transverse energy deposit of $E_{\text{T}} > 15$ GeV and some online identification criteria that are looser than the electron selection applied in the analysis.

The muon candidates are reconstructed with an algorithm which utilizes information from the silicon tracker as well as from the muon system. Background muons from cosmic rays and heavy-quark semileptonic decays are rejected by requiring a set of quality cuts on each muon based on previous studies on the performance of the muon reconstruction [24]. Electrons are reconstructed by matching ECAL clusters to tracks measured in the silicon tracker. This matching is used to differentiate electrons from photons [25]. The identification criteria are chosen to match the ones tuned in pp collisions [26].

The Z boson production cross section is calculated using the following equation:

$$\sigma = \frac{S - B}{\alpha \cdot (\epsilon \cdot \text{SF}) \cdot L_{\text{int}}} \tag{2}$$

where S is the number of Z candidates, B is the estimated background, α is the acceptance, $(\epsilon \cdot \text{SF})$ is the efficiency corrected by data-driven scale factors and L_{int} is the integrated luminosity. The phase space region considered in the analysis is defined by $p_{\text{T}}^{\ell} > 20$ GeV/c and $|\eta_{\text{lab}}^{\ell}| < 2.4$ in order to assure that the triggers are on their efficiency plateau and to be within the geometrical coverage of the muon detectors. This fiducial region of the measurement is extrapolated to the full phase space by the acceptance correction. In the following, each component of Eq. 2 is presented and their systematic uncertainties are summarized.

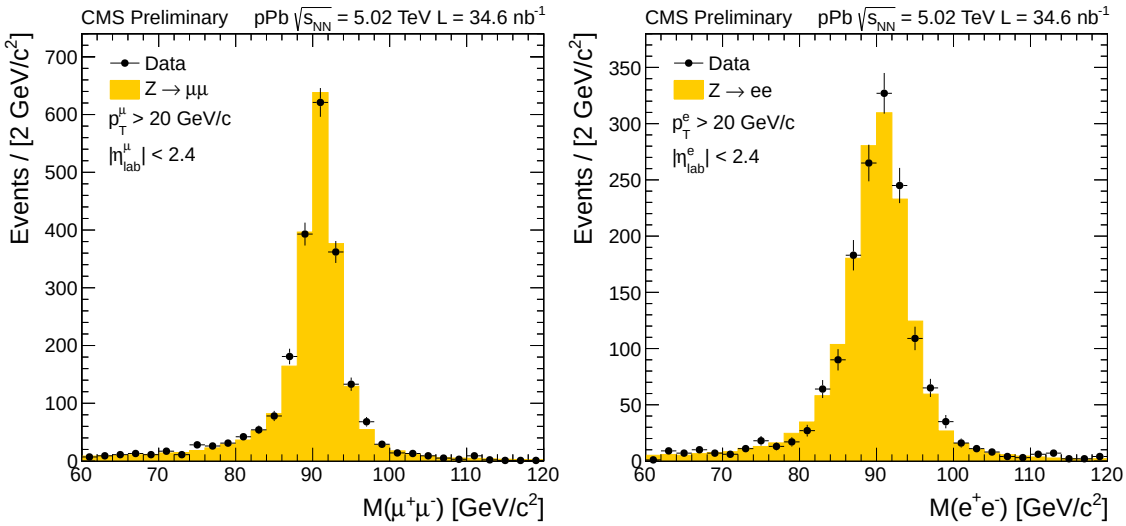

Figure 1: Invariant mass of selected muon (left) and electron (right) pairs from pPb data compared to PYTHIA 6+HIJING simulated pN $\rightarrow$ Z $\rightarrow \ell\ell$ events with N = p, n according to the number of nucleons in the Pb nucleus. The MC sample is normalized to the number of events in the data.

The Z candidate events were selected by requiring an opposite-charge lepton pair with an invariant mass in the (60-120) GeV/c^2 range, where both leptons satisfy the acceptance and quality cuts and at least one of them corresponds to the triggering signal. Figure 1 shows the invariant mass distribution of the selected lepton pairs from pPb data compared to PYTHIA 6+HIJING Monte Carlo (MC) simulation. The pN $\rightarrow$ Z $\rightarrow \ell\ell$ process is simulated using the PYTHIA 6 [27] generator (version 6.424, tune Z2) with a mixture of pp and pn interactions corresponding to pPb collisions. The detector response to each PYTHIA 6 signal event is simulated with GEANT4 [28] and then embedded in a minimum bias pPb background event. These background events are produced with the HIJING event generator [29] and then simulated with GEANT4 as well. The signal and background events share the same generated vertex location and are boosted to have the correct rapidity distribution in the laboratory frame. The embedding is done at the level of detector hits and then the events are processed through the trigger-emulation and the event-reconstruction chain. The reconstructed longitudinal primary vertex and overall multiplicity distributions are reweighted to match the ones observed in data. Energy scale and resolution corrections are applied to Z $\rightarrow$ e$^+$e$^-$ to take into account the difference between data and simulated events. Such corrections were also estimated for the Z $\rightarrow \mu^+\mu^-$ channel and found to be negligible.

The raw yield of Z boson candidates (S) in the pPb sample is determined by simply counting the number of opposite-charge lepton pairs in the 60–120 GeV/c^2 mass region that fulfill the acceptance and quality requirements. This number is found to be 2183 in the muon channel and 1571 in the electron channel. The difference between the two channels comes from the different efficiencies due to tighter selection criteria on the electrons in order to suppress the background. A charge misidentification correction of 1% is applied to the dielectron yields while it is neglibigle for dimuons. No events are found with more than one Z candidate. For the differential cross sections, the measurement is performed in the dilepton transverse momentum or rapidity bins, where the rapidity is shifted to the center-of-mass frame.

Possible background contributions to the Z $\rightarrow \ell\ell$ production are QCD multi-jet events, $t\bar{t}$ pairs

and electroweak processes such as $Z \to \tau\tau$, W+jets, diboson (WW, WZ, ZZ) production. Although the expected background contamination is small, a data-driven estimation is used to subtract the background contribution from the dilepton raw yield. For processes in which leptons result from decays involving (real or virtual) vector bosons, one expects two electron-muon events for each dimuon or dielectron event due to lepton universality. In the Z mass range, the opposite-charge electron-muon pairs are counted and translated into electron or muon pairs taking into account the differences in the electron and muon reconstruction and selection efficiencies. This background is subtracted from the dilepton raw yield and accounts for the main electroweak backgrounds, $t\bar{t}$ as well as the part of QCD background (such as $b\bar{b}$ decay) producing opposite-charge leptons. Remaining background, in particular from uncorrelated proton-nucleon collisions, is estimated by counting the same-charge lepton pairs. Additional electroweak contributions from W+jets and multi-boson production are found to be negligible by MC simulations. The fraction of background events (B) subtracted from the raw yield is 2.4% in the muon and 2.9% in the electron channel.

The efficiency for Z bosons (ϵ) is defined as the number of reconstructed Z candidates, where both leptons fulfill the acceptance and quality requirements, over the number of generated Z bosons where both leptons fulfill the acceptance cuts. This combined reconstruction, lepton identification and trigger efficiency is calculated from the PYTHIA 6+HIJING simulation samples so that the effects of the pPb environment are taken into account.

For the rapidly-falling dilepton p_{T} spectrum, an unfolding technique based on the inversion of a response matrix is first applied to the data, similar to the one used in [4], before applying the efficiency correction. This is driven by the fact that the transverse momentum resolution is not negligible compared to the analysis bin sizes. The response matrix is constructed from the PYTHIA 6+HIJING simulation to take into account the detector resolution effects and inverted to unfold the measured dilepton p_{T} distribution.

In the measurement of the dilepton rapidity, the unfolding is not necessary as the shape of the y spectrum is almost flat and the resolution is a small fraction of the analysis bin size. Instead, the efficiency corrections are calculated such that resolution effects in rapidity are taken into account. The denominator is based on the number of generated dilepton events that pass the acceptance requirements, whereas the numerator is based on the number of reconstructed dilepton events after applying the selection criteria to the dilepton reconstructed quantities and binning in reconstructed rapidity.

In order to correct for possible differences between data and simulation, a data-driven method is used to determine correction factors to the baseline efficiency from simulation. These correction scale factors (SF) are determined by applying the *tag-and-probe* method on both data and simulation to calculate single lepton efficiencies for reconstruction, identification and triggering, similar to the method described in Ref. [24]. The ratio of each efficiency from data and simulation is then applied to reweight the simulation on a lepton-by-lepton basis. The efficiency for Z bosons after taking into account the degree of agreement between simulation and data $(\epsilon \cdot \mathrm{SF})$ is found to be 0.878 in the dimuon and 0.605 in the dielectron decay channel.

The acceptance (α) is defined as the number of generated dileptons where both leptons fulfill the acceptance cuts ($p_{\mathrm{T}}^{\ell} > 20$ GeV/c, $|\eta_{\mathrm{lab}}^{\ell}| < 2.4$) over the number of all generated dileptons in the 60–120 GeV/c^2 mass region. The acceptance as a function of Z boson rapidity and transverse momentum is calculated using simulation. The event generation is provided by the POWHEG generator [30] with CT10NLO free proton PDF set [31], interfaced with PYTHIA 6 parton shower and boosted to the laboratory frame. Final-state photon radiation (FSR) is also simulated by PYTHIA 6. The integrated acceptance is found to be 0.516.

The total systematic uncertainty on the Z boson production cross section is calculated by adding in quadrature the different contributions from the background subtraction, acceptance and efficiency determination and the unfolding technique. The integrated luminosity, calibrated by the Van der Meer scans [23], has a systematic uncertainty of 3.5%. This is the dominant systematic uncertainty of the measurement in the fiducial region and is shown separately.

The raw yield of Z candidates suffers from the uncertainty of the background subtraction method. The number of subtracted background events determined by the electron-muon method is varied by $\pm$100% to assign an uncertainty on the signal yield. The uncertainty on the inclusive yield from this background variation is 1.7% in the muon and 1.8% in the electron channel.

The uncertainty on the correction factor for the electron energy scale is propagated as a systematic uncertainty on the dielectron yield. It is estimated to be 0.5% on the inclusive yield and varies with Z boson p_{T} between 4–19%. The residual difference of the mass resolution between data and simulation is taken as the systematic uncerainty in the electron channel. After propagating to the inclusive cross section it accounts for 1.1% uncertainty.

The uncertainty of the acceptance correction is estimated by changing the shape of the generated rapidity and p_{T} distributions of the Z bosons to cover differences in PDFs and possible nuclear effects. The generated dilepton rapidity is varied linearly by $\pm$30% in the $-3 < y_{c.m.} < 3$ range and the generated dilepton transverse momentum is varied linearly by $\pm$10% in the $0 < p_{\mathrm{T}} < 150$ GeV/c range when estimating the uncertainty of the acceptance. These variations cover the predicted nuclear effects to the rapidity and p_{T} spectrum from different groups [17, 18, 20] as well as the statistical uncertainties of the present measurement. The resulting uncertainty on the total acceptance is about 5% due to the extrapolation to the most forward and backward rapidity regions.

The systematic uncertainty of the efficiency comes from two different sources. First is the uncertainty of the underlying rapidity and transverse momentum distributions due to poorly known PDFs, hence their shape is varied with the same functions as for the acceptance resulting in a 0.2% uncertainty on the dilepton efficiency. Second, the statistical uncertainty of the correction factors from the ratio of data and simulation in the tag-and-probe method is propagated to the dilepton efficiency. In addition, the tag-and-probe technique employed carries itself an uncertainty of about 1% from differences observed in the efficiencies by varying the functional form or the range of the fit. Finally, the uncertainties from the three different components of the efficiency are combined in quadrature resulting in an overall uncertainty on the dimuon (dielectron) efficiency of 1.7% (2.5%).

All the uncertainties above are evaluated in bins of dilepton rapidity and p_{T} for the differential cross sections. The uncertainty of the forward-backward ratio is calculated by evaluating the variations of the background subtracted yield, the acceptance and the efficiency as described for the inclusive quantities. The combined systematic uncertainty on the forward-backward ratio ranges from 0.7% to 3.0%.

There is an additional uncertainty on the p_{T} spectrum coming from the matrix inversion procedure. The uncertainty is determined by varying the generated dilepton p_{T} distribution and the single lepton p_{T} resolution. The reconstructed p_{T} distributions from PYTHIA 6+HIJING and POWHEG+PYTHIA 6 as well as the weighted p_{T} spectrum accounting for possible nPDF differences were all probed and the effect on the results is directly evaluated. The two sources give a combined uncertainty on the unfolded yield of about 1–5% depending on the p_{T} bin.

3 Results

The Z boson production cross section is calculated using Eq. 2 for both decay channels. The analysis of the muon channel results in a fiducial cross section of 70.1 ± 1.5(stat.) $\pm$ 1.7(syst.) $\pm$ 2.5(lumi.) nb and the electron channel gives 73.9 ± 1.9(stat.) ± 2.8(syst.) ± 2.6(lumi.) nb.

The muon and electron results agree within statistical and systematic uncertainties thus a combination can be performed separating the uncertainty due to the integrated luminosity. The combination in the fiducial region is quite simple because the electron and muon samples are statistically independent and the sources of systematic errors are different. The BLUE technique [32] can be applied taking the muon and electron channel cross sections and their uncertainties uncorrelated in each bin.

The measured inclusive Z boson production cross section in the fiducial region, where both leptons fulfill the acceptance cuts is

$$\sigma_{\mathrm{pPb}\to \mathrm{Z}\to\ell\ell}(p_{\mathrm{T}}^{\ell} > 20 \text{ GeV}/c, |\eta_{\mathrm{lab}}^{\ell}| < 2.4) = 71.3 \pm 1.2(\text{stat.}) \pm 1.5(\text{syst.}) \pm 2.5(\text{lumi.}) \text{ nb}. \quad (3)$$

The prediction of the NLO calculation from POWHEG+PYTHIA 6 gives a pp cross section at 5.02 TeV of 338 ± 17 pb for $\mathrm{Z} \to \ell\ell$ production in the 60–120 GeV/c^2 mass range and applying the acceptance cuts on the leptons. Scaling this number by the number of nucleons in the Pb nucleus ($A = 208$), for pPb collisions one gets 70.4 ± 3.5 nb, which is consistent with the measured value. The pp theory prediction uncertainties come from missing higher order corrections and from the uncertainties in the PDF sets.

For the acceptance corrected total cross section, the systematic uncertainty of the acceptance is correlated between the two decay channels that is taken into account in the BLUE method. The combined total Z boson production cross section is

$$\sigma_{\mathrm{pPb}\to \mathrm{Z}\to\ell\ell} = 138.1 \pm 2.4(\text{stat.}) \pm 8.6(\text{syst.}) \pm 4.8(\text{lumi.}) \text{ nb}. \quad (4)$$

This measurement suffers from the extrapolation of the detector acceptance to the full phase space, which has an uncertainty of about 5%. The prediction from the POWHEG+PYTHIA 6 generator after scaling gives 136.1 ± 6.8 nb, which is consistent with the measured value.

Figure 2 shows the differential cross section of Z bosons in pPb collisions as a function of rapidity compared to predictions from POWHEG+PYTHIA 6 generator in the fiducial region and to MCFM generator in the full phase space. The MCFM predictions are calculated with MSTW2008NLO [33] free proton PDF set. The $\mathrm{pp} \to \mathrm{Z} \to \ell\ell$ process is simulated without nuclear modification and the $\mathrm{pN} \to \mathrm{Z} \to \ell\ell$ process is simulated with nuclear modification from EPS09 [13] and DSSZ [12] nuclear PDF sets. The theory predictions are scaled by $A = 208$. The 5% theoretical uncertainty and the luminosity normalization uncertainty of 3.5% are shown as different bands on the bottom panel of Figure 2. The measured differential cross section is consistent with the theory predictions within uncertainties that are dominated entirely by the statistical uncertainty.

Nuclear effects are expected to modify the rapidity distribution asymmetrically and thus they can be quantified by the forward-backward ratio defined in Eq. (1). This quantity is expected to be more sensitive to nuclear effects [20] because normalization uncertainties cancel both in theory and in experiment. Figure 3 shows the measured forward-backward ratio as a function

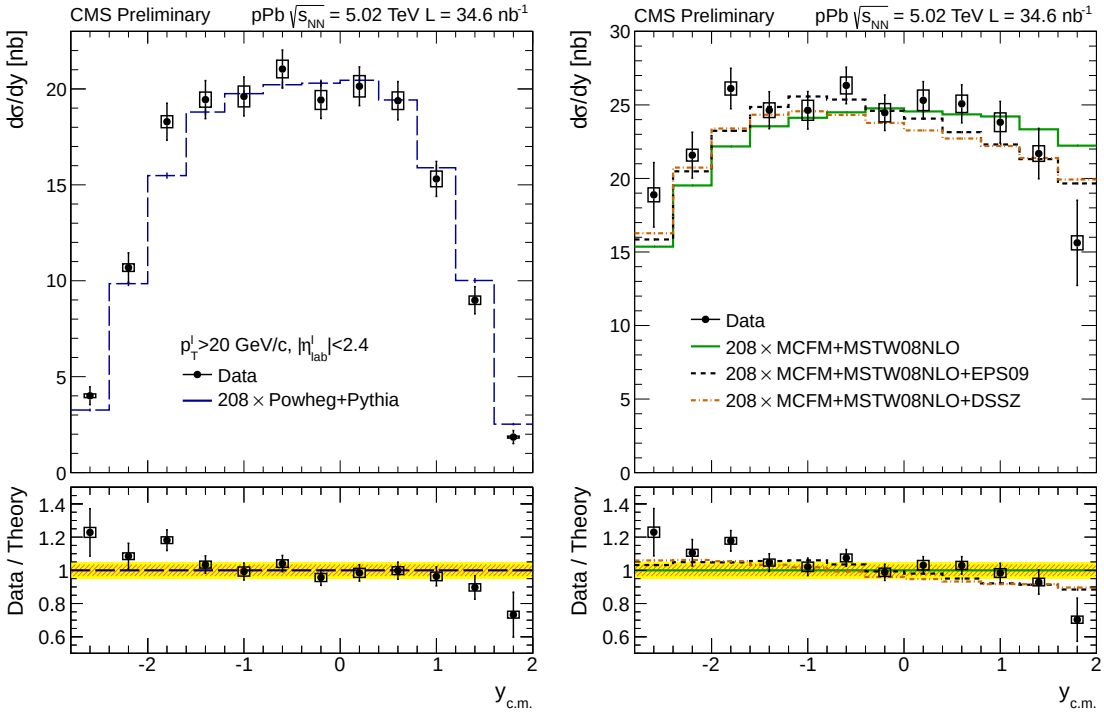

Figure 2: Differential cross section of Z bosons in pPb collisions as a function of rapidity in the fiducial region (left) and corrected to full acceptance (right) for the combined leptonic decay channel compared to predictions from POWHEG+PYTHIA 6 and MCFM generators scaled by the number of nucleons in the Pb nucleus. The 3.5% luminosity uncertainty is shown in the ratio plot as a hashed band together with the assumed 5% theoretical uncertainty shown as a yellow band.

of $|y_{\text{c.m.}}|$ compared to the POWHEG+PYTHIA 6 and the MCFM predictions with and without the nuclear modification from EPS09 or DSSZ nPDF sets.

The data has a preference to agree with the presence of nuclear effects in PDFs and together with the measured W production in pPb collisions [16], it can constrain the nPDF uncertainties by adding new data to the global fits in a previously unexplored region of the $Q^2 - x$ phase space. However, due to the large statistical uncertainties, this measurement is not able to distinguish between different nuclear PDF sets.

Figure 4 shows the differential cross section as a function of p_{T} in the fiducial and the full phase space region. The results are compared only to scaled pp theoretical predictions from POWHEG+PYTHIA 6 with CT10NLO PDF, because the expected nuclear modification of the p_{T} spectrum is small compared to the uncertainties of the theory [17, 18].

No large deviations are found from the pp theory cross sections scaled by the number of nucleons in the Pb nucleus. The difference from POWHEG+PYTHIA 6 observed in the lowest dilepton p_{T} bins is similar to the observed differences in the pp measurements at 7 or 8 TeV [2, 4].

4 Summary

The Z boson production cross section has been measured in the muon and electron decay channels in pPb collisions at $\sqrt{s_{NN}} = 5.02$ TeV. The inclusive cross sections are in agreement with

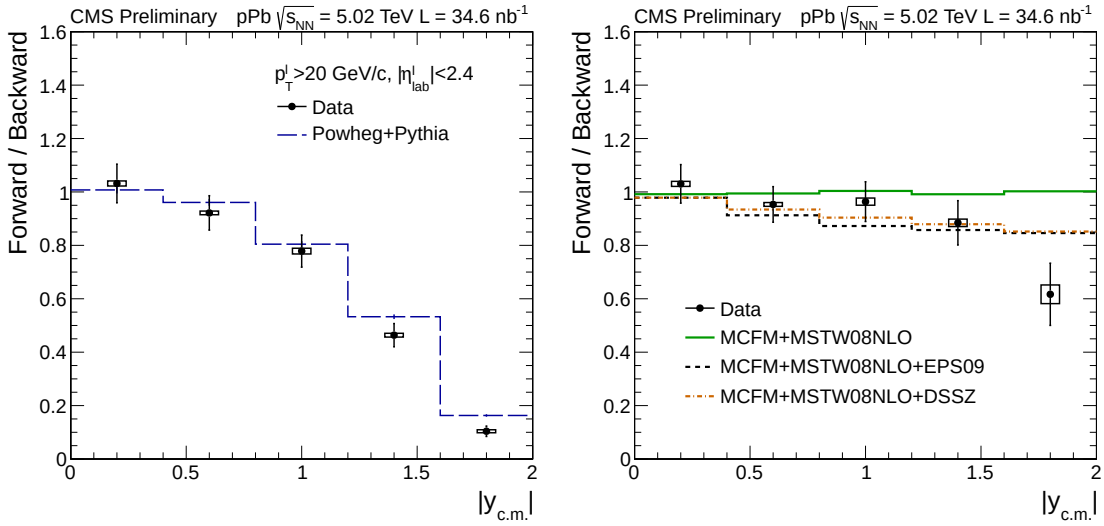

Figure 3: Forward-backward asymmetry distributions of Z bosons in pPb collisions as a function of rapidity in the fiducial region (left) and corrected to full acceptance (right) for the combined leptonic decay channel compared to predictions from POWHEG+PYTHIA 6 and MCFM generators.

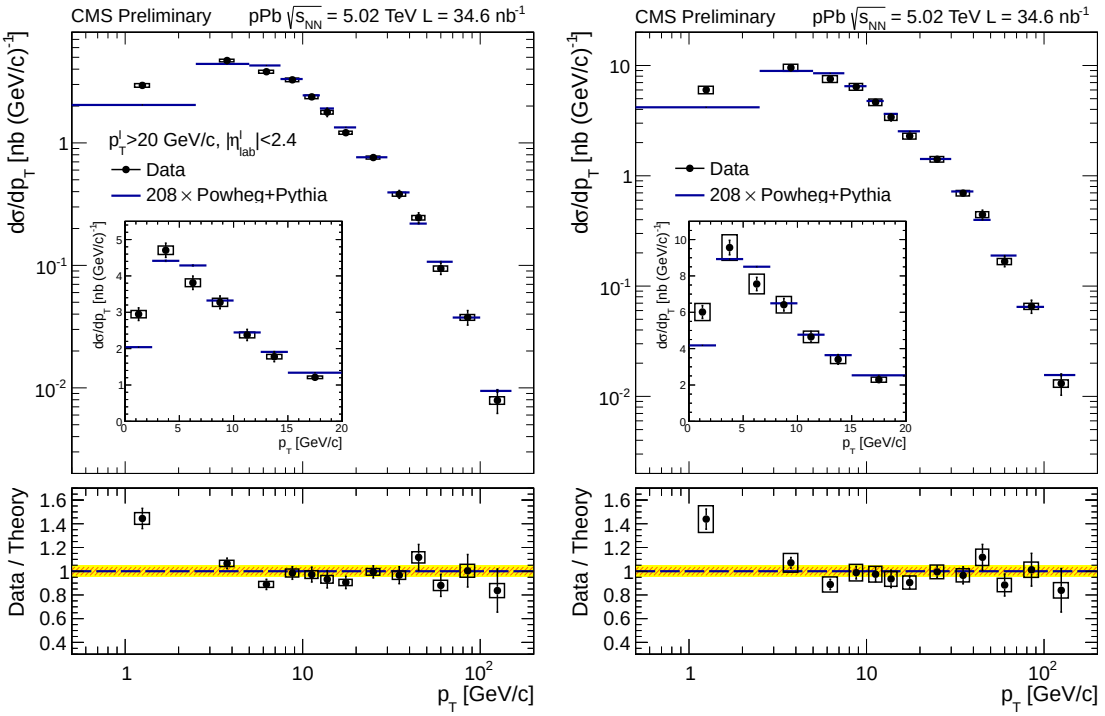

Figure 4: Differential cross section of Z bosons in pPb collisions as a function of transverse momentum in the fiducial region (left) and corrected to full acceptance (right) for the combined leptonic decay channel compared to predictions from POWHEG+PYTHIA 6 generator scaled by the number of nucleons in the Pb nucleus. The 3.5% luminosity uncertainty is shown in the ratio plot as a hashed band together with the assumed 5% theoretical uncertainty shown as a yellow band.

NLO theoretical predictions from POWHEG+PYTHIA 6 pp simulation scaled by the number of elementary nucleon-nucleon collisions. The differential cross section as a function of Z boson rapidity is consistent with the theory predictions. At large rapidity, the forward-backward ratio deviates from unity by an amount which is compatible with EPS09 and DSSZ nPDF modifications, though the statistical precision of the measurement prevents making a definitive statement. The differential cross section as a function of Z boson transverse momentum has been measured and apart from very low transverse momenta it is in fairly good agreement with the predictions from POWHEG+PYTHIA 6. The results of the presented measurement together with the measured W boson production provide new data in a previously unexplored region of phase space for constraining nuclear PDF fits.

References

[1] ATLAS Collaboration, "Measurement of the inclusive $W^{\pm}$ and Z/gamma cross sections in the electron and muon decay channels in pp collisions at $\sqrt{s} = 7$ TeV with the ATLAS detector", *Phys. Rev. D* **85** (2012) 072004, doi:10.1103/PhysRevD.85.072004, arXiv:1109.5141.

[2] ATLAS Collaboration, "Measurement of the transverse momentum distribution of Z/gamma* bosons in proton-proton collisions at $\sqrt{s} = 7$ TeV with the ATLAS detector", *Phys. Lett. B* **705** (2011) 415, doi:10.1016/j.physletb.2011.10.018, arXiv:1107.2381.

[3] CMS Collaboration, "Measurement of inclusive W and Z boson production cross sections in pp collisions at $\sqrt{s}$ = 8 TeV", *Phys. Rev. Lett.* **112** (2014) 191802, doi:10.1103/PhysRevLett.112.191802, arXiv:1402.0923.

[4] CMS Collaboration, "Measurement of the Rapidity and Transverse Momentum Distributions of Z Bosons in pp Collisions at $\sqrt{s} = 7$ TeV", *Phys. Rev. D* **85** (2012) 032002, doi:10.1103/PhysRevD.85.032002, arXiv:1110.4973.

[5] CMS Collaboration, "Measurement of the Inclusive W and Z Production Cross Sections in pp Collisions at $\sqrt{s} = 7$ TeV", *JHEP* **1110** (2011) 132, doi:10.1007/JHEP10(2011)132, arXiv:1107.4789.

[6] LHCb Collaboration, "Measurement of the cross-section for $Z \to e^+e^-$ production in pp collisions at $\sqrt{s} = 7$ TeV", *JHEP* **1302** (2013) 106, doi:10.1007/JHEP02(2013)106, arXiv:1212.4620.

[7] LHCb Collaboration, "Inclusive W and Z production in the forward region at $\sqrt{s} = 7$ TeV", *JHEP* **1206** (2012) 058, doi:10.1007/JHEP06(2012)058, arXiv:1204.1620.

[8] ATLAS Collaboration, "Measurement of Z boson Production in Pb+Pb Collisions at $\sqrt{s_{NN}} = 2.76$ TeV with the ATLAS Detector", *Phys. Rev. Lett.* **110** (2013) 022301, doi:10.1103/PhysRevLett.110.022301, arXiv:1210.6486.

[9] ATLAS Collaboration, "Measurement of the production and lepton charge asymmetry of W bosons in Pb+Pb collisions at $\sqrt{s_{\rm NN}} = 2.76$ *TeV* with the ATLAS detector", *Eur. Phys. J. C* **75** (2015) 23, doi:10.1140/epjc/s10052-014-3231-6, arXiv:1408.4674.

[10] CMS Collaboration, "Study of Z production in PbPb and pp collisions at $\sqrt{s_{\rm NN}} = 2.76$ TeV in the dimuon and dielectron decay channels", *JHEP* **1503** (2015) 022, doi:10.1007/JHEP03(2015)022, arXiv:1410.4825.

[11] CMS Collaboration, "Study of W boson production in PbPb and pp collisions at $\sqrt{s_{NN}} = 2.76$ TeV", *Phys. Lett. B* **715** (2012) 66, doi:10.1016/j.physletb.2012.07.025, arXiv:1205.6334.

[12] D. de Florian, R. Sassot, P. Zurita, and M. Stratmann, "Global Analysis of Nuclear Parton Distributions", *Phys. Rev. D* **85** (2012) 074028, doi:10.1103/PhysRevD.85.074028, arXiv:1112.6324.

[13] K. Eskola, H. Paukkunen, and C. Salgado, "EPS09: A New Generation of NLO and LO Nuclear Parton Distribution Functions", *JHEP* **0904** (2009) 065, doi:10.1088/1126-6708/2009/04/065, arXiv:0902.4154.

[14] M. Hirai, S. Kumano, and T.-H. Nagai, "Determination of nuclear parton distribution functions and their uncertainties in next-to-leading order", *Phys. Rev. C* **76** (2007) 065207, doi:10.1103/PhysRevC.76.065207, arXiv:0709.3038.

[15] C. A. Salgado, "The physics potential of proton-nucleus collisions at the TeV scale", *J. Phys. G* **38** (2011) 124036, doi:10.1088/0954-3899/38/12/124036, arXiv:1108.5438.

[16] CMS Collaboration, "Study of W boson production in pPb collisions at $\sqrt{s_{\mathrm{NN}}}$ = 5.02 TeV", arXiv:1503.05825.

[17] V. Guzey et al., "Massive neutral gauge boson production as a probe of nuclear modifications of parton distributions at the LHC", *Eur. Phys. J. A* **49** (2013) 35, doi:10.1140/epja/i2013-13035-6, arXiv:1212.5344.

[18] Z.-B. Kang and J.-W. Qiu, "Nuclear modification of vector boson production in proton-lead collisions at the LHC", *Phys. Lett. B* **721** (2013) 277, doi:10.1016/j.physletb.2013.03.030, arXiv:1212.6541.

[19] V. Kartvelishvili, R. Kvatadze, and R. Shanidze, "On Z and Z + jet production in heavy ion collisions", *Phys. Lett. B* **356** (1995) 589, doi:10.1016/0370-2693(95)00865-I, arXiv:hep-ph/9505418.

[20] H. Paukkunen and C. A. Salgado, "Constraints for the nuclear parton distributions from Z and W production at the LHC", *JHEP* **1103** (2011) 071, doi:10.1007/JHEP03(2011)071, arXiv:1010.5392.

[21] R. Vogt, "Shadowing effects on vector boson production", *Phys. Rev. C* **64** (2001) 044901, doi:10.1103/PhysRevC.64.044901, arXiv:hep-ph/0011242.

[22] CMS Collaboration, "The CMS experiment at the CERN LHC", *JINST* **3** (2008) S08004, doi:10.1088/1748-0221/3/08/S08004.

[23] CMS Collaboration, "Luminosity Calibration for the 2013 Proton-Lead and Proton-Proton Data Taking", CMS Physics Analysis Summary CMS-PAS-LUM-13-002, 2014.

[24] CMS Collaboration, "Performance of CMS muon reconstruction in pp collision events at $\sqrt{s} = 7$ TeV", *JINST* **7** (2012) P10002, doi:10.1088/1748-0221/7/10/P10002, arXiv:1206.4071.

[25] CMS Collaboration, "Energy Calibration and Resolution of the CMS Electromagnetic Calorimeter in pp Collisions at $\sqrt{s} = 7$ TeV", *JINST* **8** (2013) P09009, doi:10.1088/1748-0221/8/09/P09009, arXiv:1306.2016.

[26] CMS Collaboration, "Performance of electron reconstruction and selection with the CMS detector in proton-proton collisions at $\sqrt{s} = 8$ TeV", arXiv:1502.02701.

[27] T. Sjöstrand, S. Mrenna, and P. Skands, "PYTHIA 6.4 physics and manual", *JHEP* **05** (2006) 026, doi:10.1088/1126-6708/2006/05/026, arXiv:hep-ph/0603175.

[28] GEANT4 Collaboration, "GEANT4: A Simulation toolkit", *Nucl. Instrum. Meth. A* **506** (2003) 250, doi:10.1016/S0168-9002(03)01368-8.

[29] M. Gyulassy and X.-N. Wang, "HIJING 1.0: A Monte Carlo program for parton and particle production in high-energy hadronic and nuclear collisions", *Comput. Phys. Commun.* **83** (1994) 307, doi:10.1016/0010-4655(94)90057-4, arXiv:nucl-th/9502021.

[30] S. Alioli, P. Nason, C. Oleari, and E. Re, "NLO vector-boson production matched with shower in POWHEG", *JHEP* **0807** (2008) 060, doi:10.1088/1126-6708/2008/07/060, arXiv:0805.4802.

[31] H.-L. Lai et al., "New parton distributions for collider physics", *Phys. Rev. D* **82** (2010) 074024, doi:10.1103/PhysRevD.82.074024, arXiv:1007.2241.

[32] L. Lyons, D. Gibaut, and P. Clifford, "How to Combine Correlated Estimates of a Single Physical Quantity", *Nucl.Instrum.Meth.* **A270** (1988) 110, doi:10.1016/0168-9002(88)90018-6.

[33] A. Martin, W. Stirling, R. Thorne, and G. Watt, "Parton distributions for the LHC", *Eur. Phys. J. C* **63** (2009) 189, doi:10.1140/epjc/s10052-009-1072-5, arXiv:0901.0002.